

# Temporal variability of oceanic $\text{CO}_2$ uptake

$F\text{CO}_2$  is set by  $\Delta p\text{CO}_2 = p\text{CO}_2 - p\text{CO}_{2,\text{atm}}$

... and given the well-known atmospheric  $\text{CO}_2$  concentration we here identify seawater  $p\text{CO}_2$  discrepancies between state-of-the-art CMIP6 models and gridded  $p\text{CO}_2$ -products (SeaFlux, Fay et al., 2021).

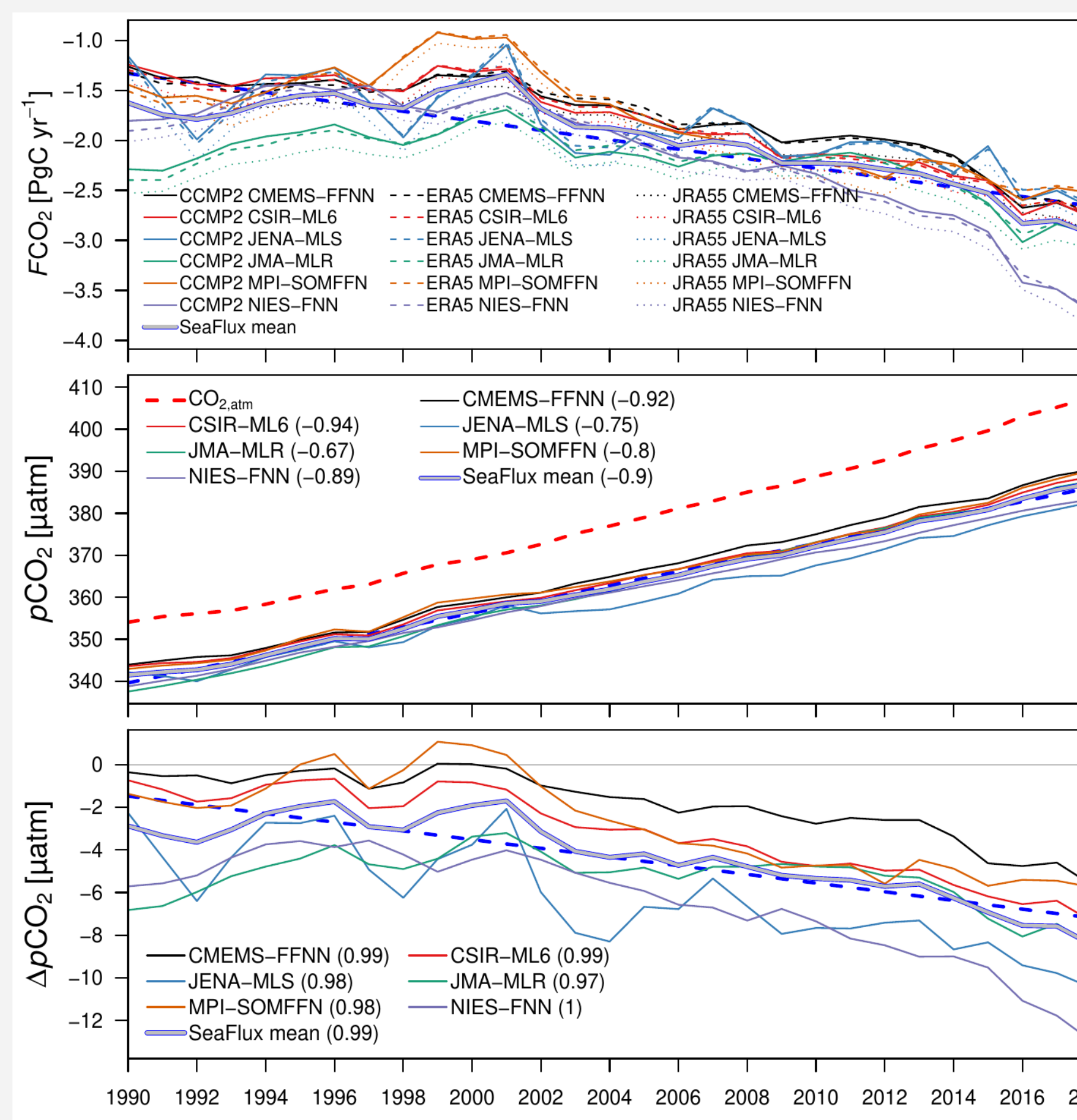
This is of importance since the ocean takes up ~25% of anthropogenic emissions since 1850 (Friedlingstein et al., 2023).

In addition to available CMIP6 data, we here present results from the global coupled climate model

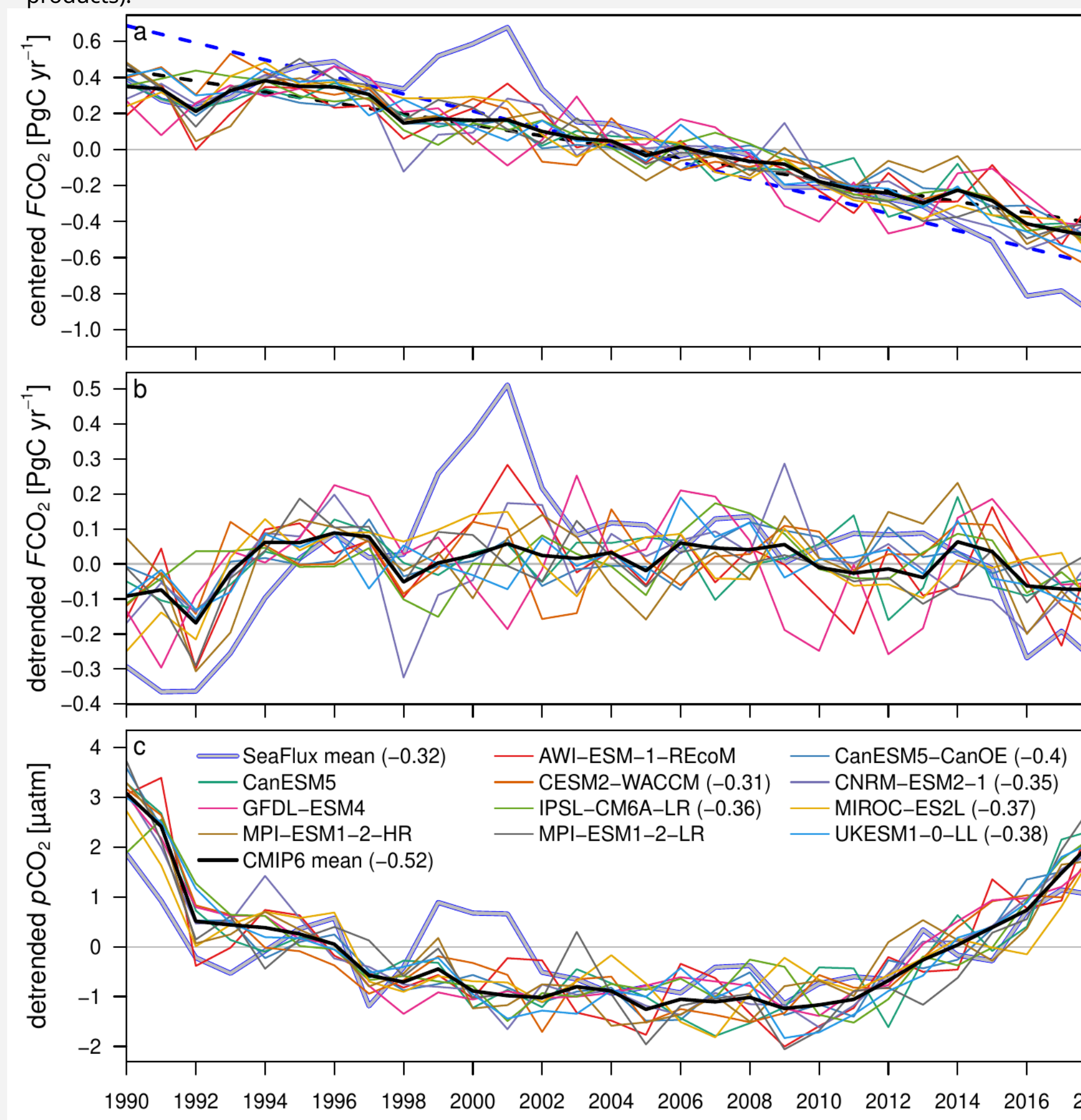
AWI-ESM-1-REcOm that simulates atmosphere, ocean and sea ice physics as well as the ocean biogeochemistry with the Regulated Ecosystem Model version 2 (REcOM; Hauck et al., 2013; Schouren-Kristensen et al., 2014).

**REcOM**  
Regulated  
Ecosystem Model

Temporal  $p\text{CO}_2$  variability is obtained by detrending globally and regionally averaged time series, i.e. removing their linear temporal trends (e.g. DeVries, 2022).



↑ Annual mean globally integrated  $F\text{CO}_2$  (a) and averaged  $p\text{CO}_2$  (b) and  $\Delta p\text{CO}_2$  (c) from SeaFlux (Gregor and Fay, 2021), thick gray-blue line is ensemble mean, thick dashed blue line is linear trend of ensemble mean. In a, negative values denote oceanic  $\text{CO}_2$  uptake and labels refer to wind and  $p\text{CO}_2$ -products. In b, the red dashed line is the globally averaged observed atmospheric  $\text{CO}_2$  mole fraction (in ppm; Lan et al., 2023). Numbers in labels in b and c provide significant correlations with a (averaged over three wind products).



↑ Detrended annual mean  $p\text{CO}_2$  from SeaFlux ensemble mean (Gregor and Fay, 2021) and CMIP6 models averaged globally (a) and over five biomes (map in a; Gregor et al., 2019). Positive values mark years with higher  $p\text{CO}_2$  compared to the linear trend. Numbers in labels after 'C' and 'N' provide correlations with detrended annual global mean atmospheric  $\text{CO}_2$  concentration (dashed red line) (identical in all panels; Lan et al., 2023) and annual mean Niño 3.4 anomaly index (Rayner, 2003), if significant. In b, red/blue bars mark El Niño/La Niña events (Niño 3.4 index area shown by black box in map).

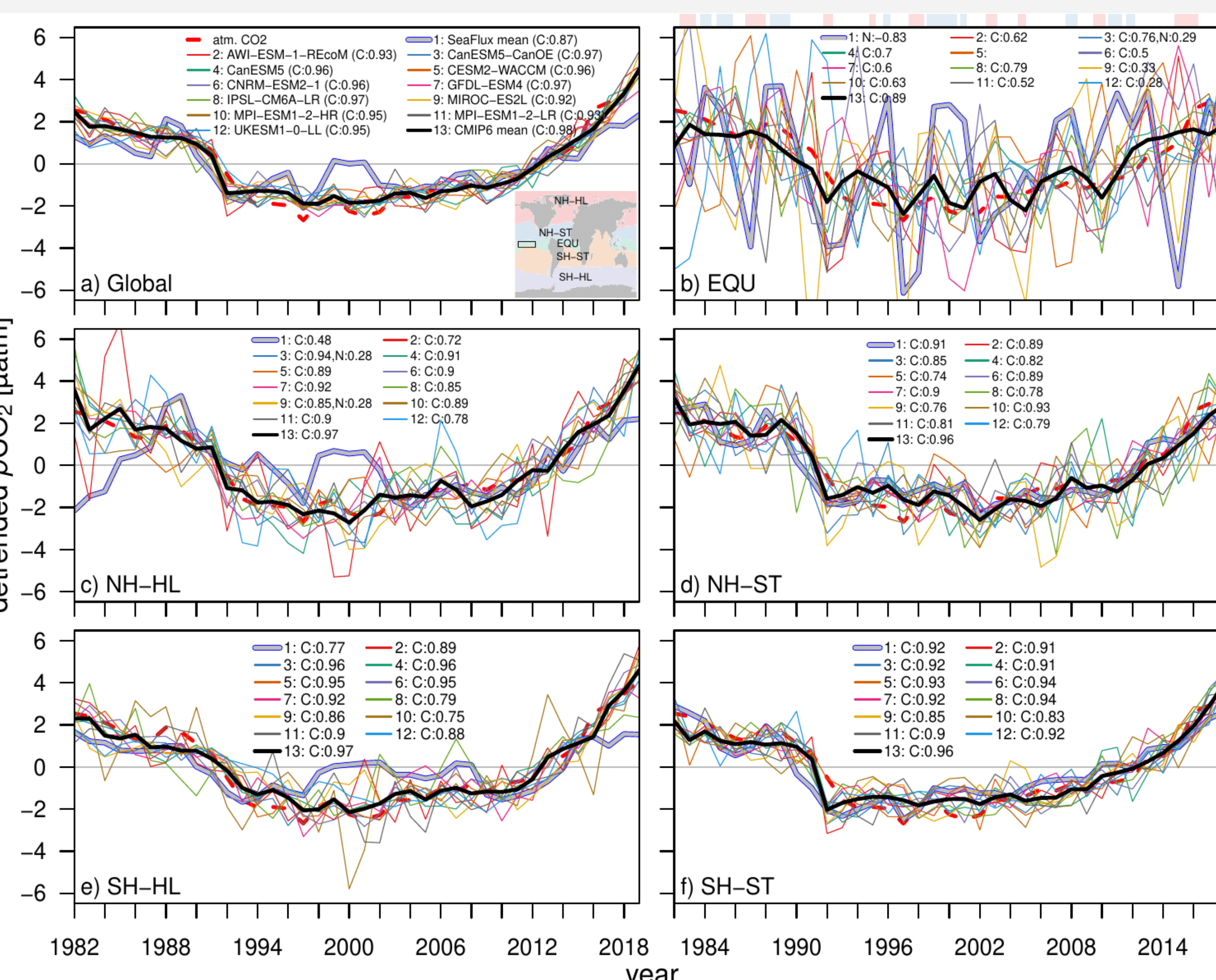
## Discrepancies in temporal $p\text{CO}_2$ variability from Earth System Models and $p\text{CO}_2$ -products related to high-latitude mixed layer dynamics and equatorial upwelling

Christopher Danek (cdanek@awi.de) and Judith Hauck

Alfred Wegener Institute for Polar and Marine Research (AWI), Am Handelshafen 12, Bremerhaven, 27570, Bremen, Germany

# But seawater $p\text{CO}_2$ variability is off in CMIP6 models in equatorial and high latitudes

The temporal variability of seawater  $p\text{CO}_2$  from the SeaFlux data product is largely determined by the atmospheric  $\text{CO}_2$  concentration (McKinley et al., 2017) and explains the slowdown and reinvigoration of  $F\text{CO}_2$  before and after the year 2000 (Gruber et al., 2023). This is especially the case in the subtropics of both hemispheres (NH-ST, SH-ST). The correlation, however, decreases in the high latitudes (NH-HL, SH-HL) and vanishes in the equatorial region (EQU).

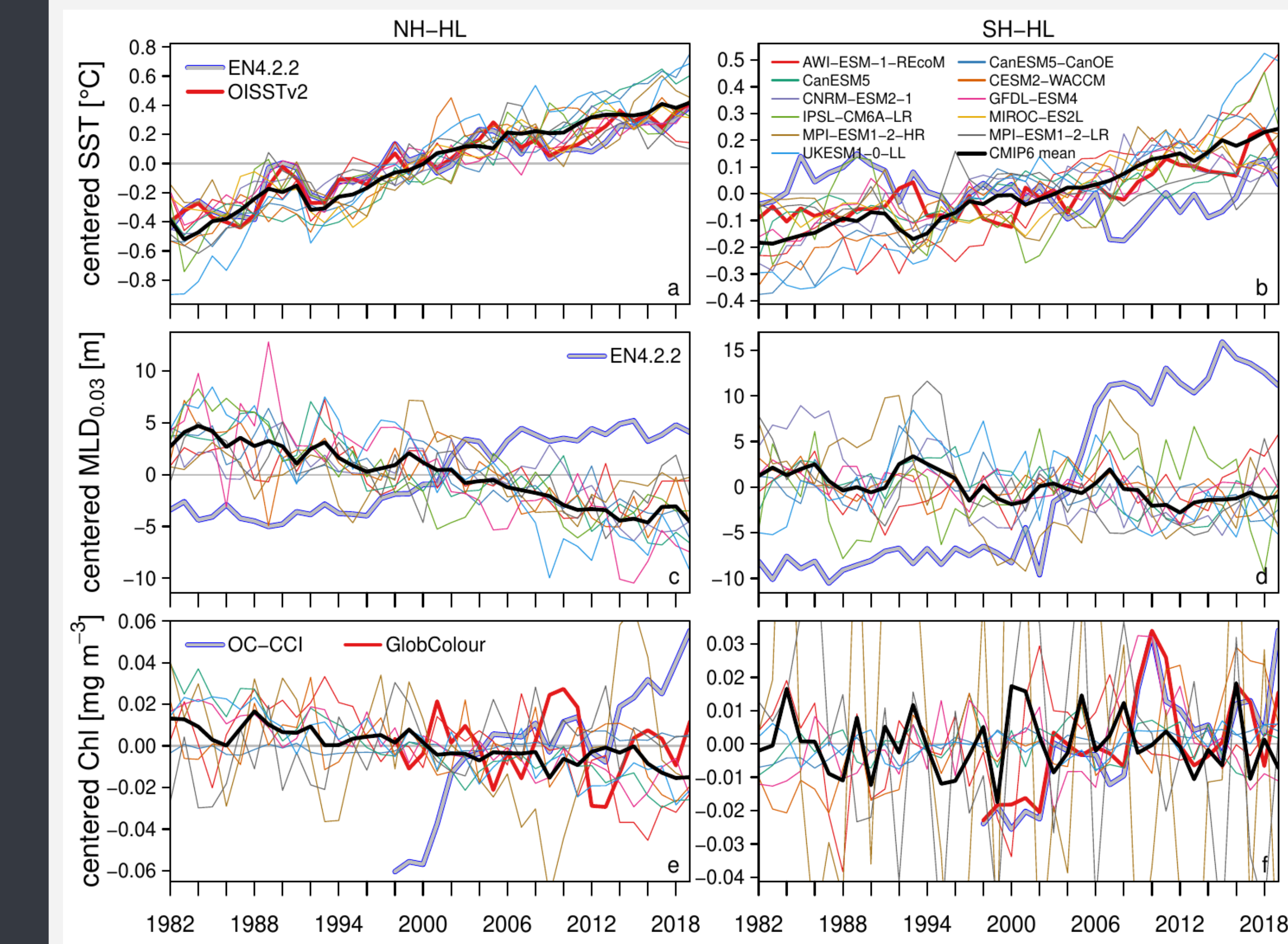


↑ Detrended annual mean  $p\text{CO}_2$  from SeaFlux ensemble mean (Gregor and Fay, 2021) and CMIP6 models averaged globally (a) and over five biomes (map in a; Gregor et al., 2019). Positive values mark years with higher  $p\text{CO}_2$  compared to the linear trend. Numbers in labels after 'C' and 'N' provide correlations with detrended annual global mean atmospheric  $\text{CO}_2$  concentration (dashed red line) (identical in all panels; Lan et al., 2023) and annual mean Niño 3.4 anomaly index (Rayner, 2003), if significant. In b, red/blue bars mark El Niño/La Niña events (Niño 3.4 index area shown by black box in map).

In EQU, instead, upwelling dynamics from ENSO induce a large temporal  $p\text{CO}_2$  variability that is misrepresented in CMIP6 models as modeled and observed sea surface temperature (SST) are generally not correlated (not shown).

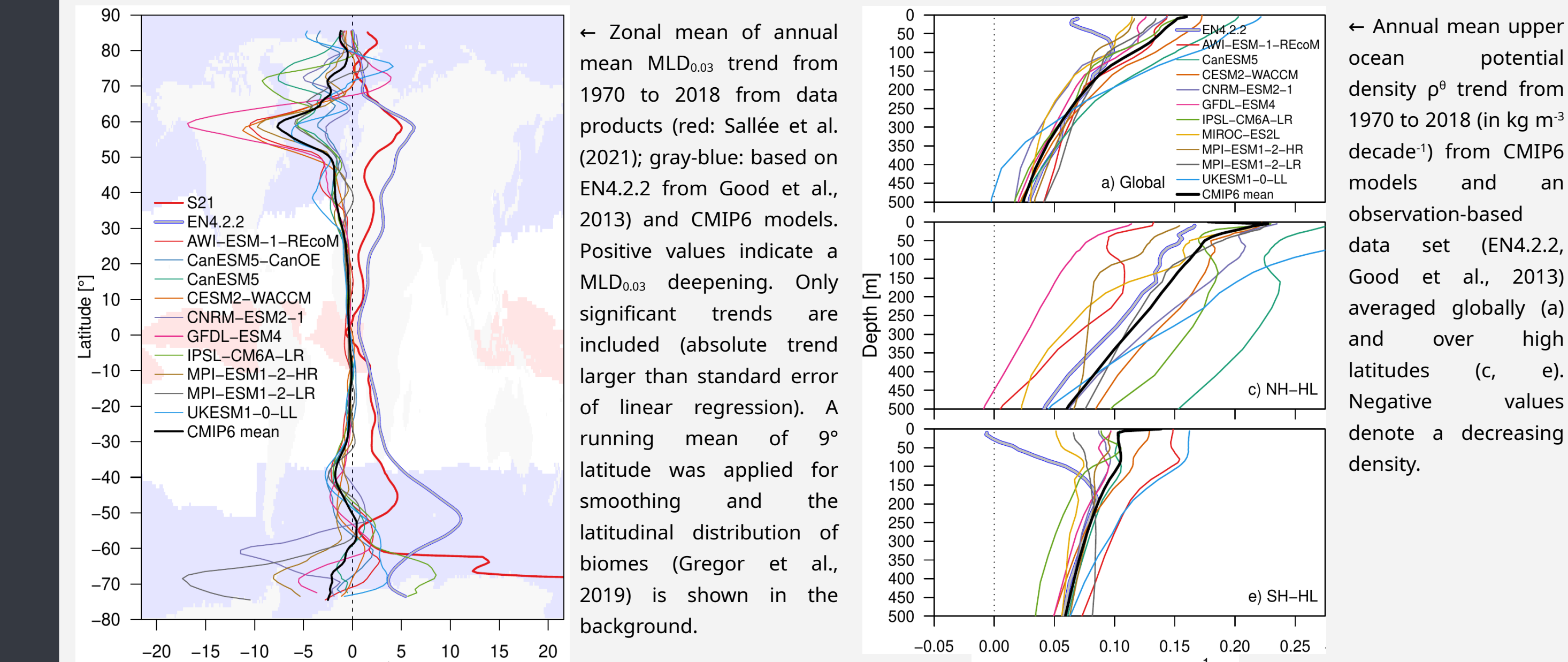
In the high latitudes, we identified large discrepancies in modeled and data product  $p\text{CO}_2$  variability, especially around the year 2000. We attribute this discrepancy to a systematic mixed layer bias in CMIP6 models, which show shallower mixed layers over the observational period, in contrast to observations (look to the right!).

# Because all CMIP6 models show a shallowing mixed layer, in contrast to observations



↑ Annual mean centered (1982–2019 mean removed) SST (top), MLD<sub>0.03</sub> (middle) and Chl (bottom) from observational data sets and CMIP6 models, spatially averaged over NH-HL (left) and SH-HL biomes (right). Positive values indicate larger than the temporal mean (deeper for MLD<sub>0.03</sub>). Data sets are OISSTv2 (Huang et al., 2021) for SST, EN4.2.2 (Good et al., 2013) for SST and MLD<sub>0.03</sub> and OC-CCI (Sathyendranath et al., 2019) and GlobColour (European Union-Copernicus Marine Service, 2022) for Chl. Some variables are not available for all models. In e and f, MPI-ESM values are not included in y-axes limits.

In the CMIP6 models, an overestimated lightening of the upper ocean induced by climate change is likely the reason for shallower mixed layers, as the vertical density profile becomes flatter. Although this mixed layer depth bias occurs at almost all latitudes, its contribution to vertical carbon supply is limited to the highly dynamic high latitudes, in contrast to the the temperature and  $\text{CO}_{2,\text{atm}}$ -driven subtropics.



← Zonal mean of annual mean MLD<sub>0.03</sub> trend from 1970 to 2018 from data products (red: Sallée et al., 2021; gray-blue: based on EN4.2.2 from Good et al., 2013) and CMIP6 models. Positive values indicate a MLD<sub>0.03</sub> deepening. Only significant trends are included (absolute trend larger than standard error of linear regression). A running mean of 9° latitude was applied for smoothing and the latitudinal distribution of biomes (Gregor et al., 2019) is shown in the background.  
← Annual mean upper ocean potential density  $p^0$  trend from 1970 to 2018 (in kg m<sup>-3</sup> decade<sup>-1</sup>) from CMIP6 models and an observation-based data set (EN4.2.2, Good et al., 2013) averaged globally (a) and over high latitudes (c, e). Negative values denote a decreasing density.



ALFRED-WEGENER-INSTITUT  
HELMHOLTZ-ZENTRUM FÜR POLAR-  
UND MEERESFORSCHUNG